PAPER • **OPEN ACCESS**

An efficient numerical integration system for stiff unified constitutive equations for metal forming applications

To cite this article: J Dear *et al* 2022 *IOP Conf. Ser.: Mater. Sci. Eng.* **1270** 012008

View the article online for updates and enhancements.

You may also like

- Effect of Electrochemically Grafted Aryl-Based Monolayer on Nonspecific Electrical Signal of Field-Effect-Transistor-Based Biosensor
Shogo Himori, Shoichi Nishitani and Toshiya Sakata
- Construction of Space Quantum Information System Based on Satellite Recognition
Lingping Tao
- Ion-selective Polymer Electrolyte Membrane Based on Sulfonated Silica and Sulfonated Poly(Phenylene Oxide) for Redox Flow Battery
Sung-Hee Roh and Ho-Young Jung

This content was downloaded from IP address 78.151.127.42 on 23/12/2022 at 11:21

An efficient numerical integration system for stiff unified constitutive equations for metal forming applications

J Dear*, Z Shi and J Lin
Department of Mechanical engineering, Imperial College London, London, SW7 2AZ, UK
* Corresponding author, E-mail: james.dear17@imperial.ac.uk

Abstract. Unified constitutive equations have been developed in recent years to predict viscoplastic flow and microstructural evolution of metal alloys for metal forming applications. These equations can be implemented into commercial FE code, such as ABAQUS and PAMSTAMP, to predict mechanical and physical properties of materials in a wide range of metal forming processes. These equations are normally stiff and need significant computer CPU time to solve. In this research, a series of numerical analyses are performed to investigate the difficulties within MATLAB of solving these stiff unified constitutive equations. A metric is introduced to allow evaluation of the numerical stiffness to assess the most appropriate numerical integration method. This metric is based on the ratio of maximum to minimum eigenvalue. This metric allows for an appropriate numerical method to be chosen giving more effective modelling of deformation and plasticity processes. Based on the theoretical work described above, a user-friendly system, based on MATLAB, is then developed for numerically integrating these types of stiff constitutive equations. This is particularly useful for metal forming engineers and researchers who need an effective computational tool to determine constitutive properties well based on numerical integration theories.

1. Introduction

Many problems in the simulation of viscoplastic flow processes for metal forming applications can be described by systems of ordinary differential equations. These problems are often multiscale and stiff and hence are only amenable to implicit solvers. Commonly used implicit solvers require extensive matrix processing whilst standard explicit methods have limited stability and progress in smaller time increments. This means the simulation of these viscoplastic flow/creep processes is computationally intensive. Consequently, improvements in numerical integration and algorithm efficiency can always be utilized. Whilst much research has been performed to solve stiff equations and a variety of implicit solvers have been developed [1-3], many more advanced recently developed numerical methods, due to their algorithmic complexity, are left unused [4-7]. In this research, several stable numerical methods are examined. The proposed algorithms are found to be best in their class, combining computational efficiency and strong stability. In addition, these methods make more efficient use of current computer resources and are particularly well suited to viscoplastic flow/creep constitutive equations, where the solution is determined implicitly by choice of the material dependent variables [8-11]. Three implicit numerical integration methods are outlined for used for numerical integrating stiff mechanism-based constitutive equations. These techniques have been recently developed to navigate more efficiently regions of numerical instability. One stiffness index or metric, based on the eigenvalues of the Jacobian matrix, has been introduced to assess localised stiffness within first order non-linear ODE systems as found for many constitutive equations. This provides an assessment of the most suitable numerical method. The main objective of this research is to provide a graphical user interface which provides

Content from this work may be used under the terms of the Creative Commons Attribution 3.0 licence. Any further distribution of this work must maintain attribution to the author(s) and the title of the work, journal citation and DOI.
Published under licence by IOP Publishing Ltd

consistent, efficient numerical integration. Additionally, functionally to add new constitutive equations, to the three embedded equation sets listed in appendix A, has been introduced, so a user/researcher can investigate any given equation set.

2. Numerical solution to ODEs

Explicit and implicit numerical integration methods are two approaches often employed in numerical analysis, for obtaining numerical solutions to first order differential equations, as often required in physical processes:

$$\dot{y} = \mathrm{f}(t, y),\ y(t_0) = y_0 \tag{1}$$

The most classical examples being the explicit and implicit Euler method [12]. The implicit Euler method is known to be most suitable for stiff constitutive equations due to improved stability. The stability of a numerical method is determined by considering the following test equation:

$$\dot{y} = \lambda_i y,\ y(0) = 1 \tag{2}$$

For $\mathrm{Re}(\lambda_i) < 0$ (real part less than zero) the solution decays exponentially fast as *t* increases. So, the performance of a method on the test equation will indicate how well, it will perform on more general systems. A method is considered A-stable if $\left|\frac{y_{k+1}}{y_k}\right| \to 0$ as k goes to infinity for all the values satisfying $\mathrm{Re}(h\lambda_i) < 0$ (real part less than zero). An L-stable method is a stronger condition than A-stability concerned with the asymptotic behaviour of the solution. Again, its definition is based on linear test problem equation (2). A method is considered L-stable if its A-stable and additionally $\left|\frac{y_{k+1}}{y_k}\right| \to 0$ as $h\lambda \to \infty$.

2.1. Implicit Euler

The implicit Euler method is usually combined with the trapezoidal rule to provide accurate error estimation [1]. The IE-TR method (Implicit Euler-Trapezoidal Rule) combines the stronger stability from the L-stable Implicit Euler method with the higher order trapezoidal rule to obtain:

$$y_{k+1} = y_k + \Delta t\ \mathrm{f}_{k+1} \tag{3}$$

$$\tilde{y}_{k+1} = y_k + \frac{\Delta t}{2}(\mathrm{f}_k + \mathrm{f}_{k+1}) \tag{4}$$

where $y_{\mathrm{k+1}}$ and $\tilde{\mathrm{y}}_{\mathrm{k+1}}$ are the numerical solutions obtained by each respective method of order one and two: $\mathrm{f_k} = \mathrm{f}(t_k, y_k)$, $\mathrm{f_{k+1}} = \mathrm{f}(t_{k+1}, y_{k+1})$ are the derivatives of the system and $\Delta\mathrm{t}$ is the time increment of the integration. The method achieves a local truncation error estimation of order one and two respectively. The leading order local truncation error is calculated as $e_k = y_{k+1} - \tilde{y}_{k+1}$ with a suitable norm applied and therefore achieves an error estimation of order one.

2.2. Rosenbrock method

Implicit methods are computationally more expensive, since one must solve the resulting non-linear difference equations. The implicit Rosenbrock method provides a compromise by reducing the computational complexity whilst still providing good accuracy and stability. The most widely used method [4] consists of two semi-implicit modified Rosenbrock methods of orders 2 and 3 (Rosenbrock-23) such method is considered a DIRK (Diagonally Implicit Runge-Kutta) and is given by:

$$k_1 = W^{-1}\mathrm{f}_k \tag{5}$$

$$k_2 = W^{-1}[\mathrm{f}_{k+0.5} - k_1] + k_1 \tag{6}$$

$$k_3 = W^{-1}[\mathrm{f}_{k+1} - c_{32}(\mathrm{k}_2 - \mathrm{f}_{k+0.5})) - 2(\mathrm{k}_1 - \mathrm{f}_k)] \tag{7}$$

$$y_{k+1} = y_k + \Delta t k_2 \tag{8}$$

where the matrix $W = I - a\Delta t\, J$ which is assumed to be invertible. This is with J the Jacobian matrix, I is the identity matrix, $a = \frac{1}{2+\sqrt{2}}$, $c_{32} = 6 + \sqrt{2}$ and $f_{k+0.5} = f(t_k + 0.5\Delta t, y_k + 0.5\Delta t\, k_1)$. The leading order local truncation error is calculated as the difference between the second and third order numerical solution and is shown below:

$$e_k \approx \frac{\Delta t}{6}(k_1 - 2k_2 + k_3) \tag{9}$$

It should be noted that the local truncation error achieves an estimation of $\mathcal{O}(\Delta t^3)$ (of order three) and the method is L-stable under a step size restriction, see [4] for a full proof. Analysis of the stability function also reveals that improved stability property is not obtained from more accurate Jacobians therefore numerical Jacobian are often employed are. Additionally, in practice the same Jacobian can be used for some subsequent steps provided the solution changes slowly.

2.3. TR-BDF2

The L-stable methods found to be most successful in this research, in dealing with systems, with severe stiffness, is the TR-BDF2 method [13]. The TR-BDF2 is defined as a composite one-step method resulting from the composition of the trapezoidal rule in the first sub-step, followed using a second-order backward differentiation formula (BDF2) method in the second sub-step. This method has been found to be particularly promising for stiff ODEs due to its strong stability (L-stability) and improved order of accuracy achieved due the use of a higher order BDF method [7]. The TR-BDF2 method is shown below:

$$y_{k+\gamma} = y_k + \gamma\frac{\Delta t}{2}(\mathrm{f}_k + \mathrm{f}_{\mathrm{k}+\gamma}) \tag{10}$$

$$y_{k+1} - \frac{1-\gamma}{2-\gamma}\Delta t\, \mathrm{f}_{k+1} = \frac{1}{\gamma(2-\gamma)}y_{k+\gamma} - \frac{(1-\gamma)^2}{\gamma(2-\gamma)}y_{\mathrm{k}} \tag{11}$$

where the parameter γ is given in the range of $\gamma \in (0,1)$ and $\mathrm{f}_{k+\gamma} = \mathrm{f}\big(t_k + \gamma\Delta t, y_{k+\gamma}\big)$. The trapezoidal rule (TR) first advances the solution to $\mathrm{t}_{\mathrm{k}+\gamma}$, an intermediate point $y_{k+\gamma}$, where $t_{k+\gamma} = t_k + \gamma\Delta t$. Secondly, the BDF2 method (equation 11) uses three contributions of points at y_k, $y_{k+\gamma}$ and y_{k+1} to advance to the final point at $\mathrm{t}_{\mathrm{k}+1}$. The leading order truncation error for the TR-BDF2 scheme [4] can be computed as:

$$e_k \approx\ 2k_\gamma\Delta t\left(\frac{1}{\gamma}\mathrm{f}_{\mathrm{k}} - \frac{1}{\gamma(1-\gamma)}\mathrm{f}_{\mathrm{k}+\gamma} + \frac{1}{(1-\gamma)}\mathrm{f}_{\mathrm{k}+1}\right) \tag{12}$$

where $k_\gamma = \frac{-3\gamma^2+4\gamma-2}{12(2-\gamma)}$. The choice of parameter of $\gamma = 2 - \sqrt{2}$ provide three overall advantages, first it minimizes the local truncation error in equation (12). see [4]. A higher order estimate of the local truncation error is achieved with this method of $\mathcal{O}(\Delta \mathrm{t}^3)$. Also, the region of absolute stability is improved as well as L-Stability. Most conveniently, the Jacobians used to converge to the solution, in trapezoid rule equation (10) and BDF scheme equation (11) are identical, reducing the complexity of solving the non-linear systems.

2.4. Error control and step size selection

The choice of error control and step-size algorithm is key to ensuring accurate numerical solutions. In numerical integrations, local truncation error is controlled, by introducing an allowable truncation error, known as the tolerance. In some cases, such as in multi-scale constitutive equations, this is difficult to introduce for every material state-variable. Therefore, many unitless errors have be developed based on the local truncation error:

$$e_k = y_{k+1} - \tilde{y}_{k+1}, \qquad r_k = \frac{e_k}{y_k}, \qquad \bar{e}_k = \frac{e_k}{\Delta y_k}$$

where $\Delta y_k = y_{k+1} - y_k$, r_k is the relative error [4] and $\bar{e}_k$ is the normalised error [1]. Additionally, these two unitless errors, based on the local truncation error provide more convenient error control within a

step-size control algorithm. In some cases, the absolute and relative error and both controlled dynamically by use of a relative Tolerance and an Absolute Tolerance. Alternatively, the normalised error first introduced in [1] allows for unitless error control based on one tolerance.

2.5. The phenomenon of numerical stiffness

Stiff systems of ordinary differential equations are a very important special case of the systems taken up in Initial Value Problems. There is no universally accepted definition of stiffness meaning it is difficult to assess. The most practical definition of stiff equations are those where certain implicit methods, in particular backward differentiation methods, perform much better than explicit ones (see [6]). Therefore, stability requirements rather than accuracy contain the step-size. The stability of a numerical method can be found by using test equation (2), where the eigenvalue of the test method uniquely defines the region of absolute stability for each numerical method. The Jacobian used within the iterative solver for each non-linear system is given by the $n \times n$ matrix:

$$J = \partial_y \mathrm{f}(t, y) = \left(\frac{\partial \mathrm{f}_i}{\partial y_j}\right) \tag{13}$$

Some attempts to understand stiffness for the system $\dot{y} = \mathrm{f}(t, y)$ therefore examine the eigenvalues of the Jacobian, λ_i since they also satisfy equation (2) meaning they determine the stability. Many definitions have been proposed to explain this phenomenon, but in practice, a stiff system occurs when some components of the solution decay more rapidly than others. This is often the case when one eigenvalue with a large negative real part exists in the system. To account for the true scale of the stiffness, a ratio is introduced. The introduced stiffness index, locally of a system, is the positive real number:

$$s = \frac{\mathrm{Re}(\lambda_{max})}{\mathrm{Re}(\lambda_{min})} \tag{14}$$

where λ_i are the eigenvalues of the Jacobian, of equation (13) and λ_{min} and λ_{max} are the smallest and largest eigenvalues with $\mathrm{Re}(\lambda_i) < 0$. This index describes the local stiffness and is helpful in assessing the most appropriate numerical method. Systems are considered stiff on the interval of $[t_0, t_{max}]$ if $S(t_0 - t_{max}) \gg 1$, as indicated in table 1.

Table 1. Stiffness level assessment and the recommendation for selecting numerical integration methods.

Stiffness Index	$S(t_0 - t_{max}) \leq 10$	$10 < S(t_0 - t_{max}) < 10^5$	$S(t_0 - t_{max}) \geq 10^5$
Classification	Not considered stiff	Mild stiffness	Severe stiffness
Suggested Outcome	Explicit methods can be used	Semi-implicit methods can be most efficient	Implicit methods can only be used

3. Numerical integration system development

The numerical integration system is developed based on the algorithms and functions available in MATLAB. Figure 1 shows the overall structure of the system, which consists of three major parts. The first part is the 'model input' where a user can input their own constitutive equations, into the system or choose from the list of embedded equations within the GUI (Graphic User Interface) allowing modelling of a wide range of metal forming conditions and materials. For the initial system development, three sets of constitutive equations listed in Appendix A have been embedded into the system for user selection. The system chooses the most appropriate numerical method to be employed or the numerical method selected by the user. Some "post processing" options have been provided to allow further analysis or export of the raw data obtained from numerical integration. Some additional analysis can also be obtained to view the performance of each numerical method, as well the accumulated error and

step-size used throughout each integration. This has been found to be useful in diagnosing difficulties in numerical integration.

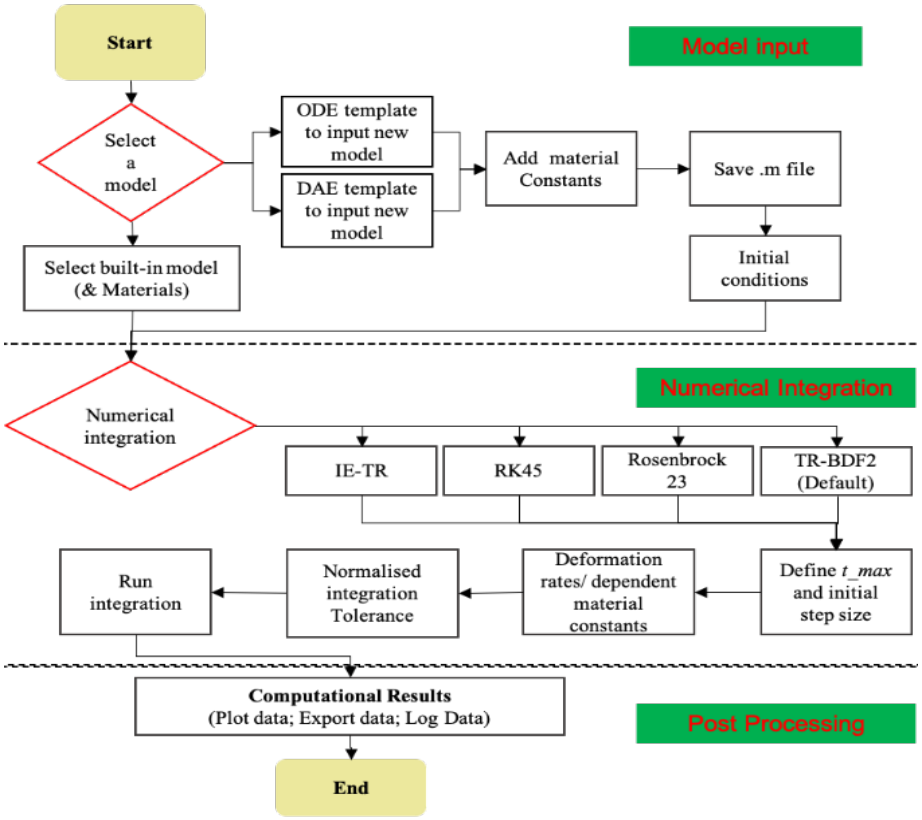

Figure 1. Structure of the numerical integration system based on the algorithms and functions available in MATLAB for integrating unified viscoplastic constitutive equations with developed GUI for pre- and post-processing.

As an example, the creep age forming equations ODE_10 (see Appendix A.2) for Aluminium alloy AA2050-T34 at 428 K [9], have been successfully numerically integrated, as shown in figure 2 where creep strain versus time (in hours) has been plotted within the interface, for four different stresses of 120, 160, 200 and 240 MPa, using the TR-BDF2 method.

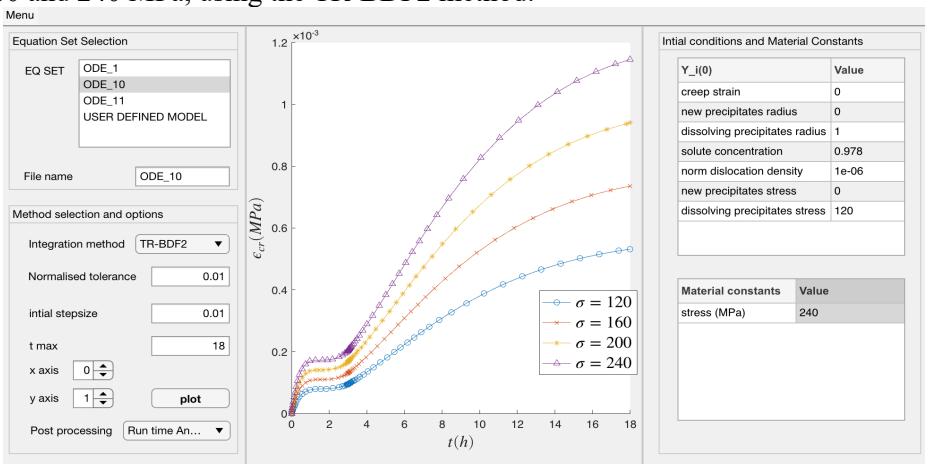

Figure 2. GUI system and computational results for creep ageing constitutive equations. Creep strain versus time (hours) for different stresses (120, 160, 200 and 240 MPa) for creep-ageing of Aluminium Alloy (AA2050-T34 at 428 K) see [9], solved using the TR-BDF2 method.

The initial values for creep strain, new precipitate radius, dissolving precipitate radius, solute concentration, normalised dislocation density, new precipitate stress and dissolving precipitate stress can be also adjusted (in appropriate units) according to requirements.

4. Conclusions

In this research, an efficient and user-friendly numerical integration system is established based on the available numerical algorithms and functions in MATLAB for solving unified viscoplastic constitutive equations in metal forming applications. The user-friendly graphical interface has been developed, which enables users to define constitutive equations which are then input into the system. The system has been tested by users, who are not familiar with numerical integration theories, and very encouraging comments have been received.

Appendix A: List of unified constitutive equations used for the system development

SET 1: General viscoplastic constitutive equations
During warm metal forming processes, the workpiece/material is deformed viscoplastically. To model the elastic–viscoplastic deformation and material hardening, the following set of constitutive equations is proposed and determined for micro-alloyed air-quenched steel in warm/hot forming:

$$\left.\begin{aligned} \dot{\varepsilon}_p &= \left(\frac{\sigma-R-k}{K}\right)_+^n \\ \dot{\bar{\rho}} &= A(1-\bar{\rho})\dot{\varepsilon}_p - C\bar{\rho}^{\gamma_0} \\ \dot{\sigma} &= E\left(\dot{\varepsilon}_T - \dot{\varepsilon}_p\right) \end{aligned}\right\} \quad (A.1)$$

Where $(-)_+$ ensures the base is positive; where $R = B\bar{\rho}^{\frac{1}{2}}$ is isotropic hardening, where E is the Young's modulus with $E = 110$ GPa (at a temperature of 850 $^{\circ}C$). The material constants of the system are *k, K, n, A, C,* γ_0 and *B*. The equation set was determined for micro-alloyed air-quenching steel in warm forming conditions and the material constants within the equations are listed in table A1 [1].

Table A1. Determined material constants used to model elastic-viscoplastic deformation and material hardening of micro-alloyed steel.

k (MPa)	K (MPa)	n (-)	A (-)	C (s^{-1})	γ_0 (-)	B (MPa)
0.34	51.67	1.31	10.49	0.25	1.01	200.18

The initial conditions for this model involving micro-alloyed steel are given by: $\varepsilon_p(0) = 0$, $\bar{\rho}(0) = 0$ and $\sigma(0) = 0$.

SET 2: Creep ageing constitutive equation
The constitutive model for creep-ageing of aluminium alloy AA2050-T34 was proposed in [9] where the creep strain rate is controlled by an applied stress, as well as the increasing dislocation density, dissolving precipitates, other metallurgical/microstructural features in the metallic alloys and temperature. As shown below:

$$\left.\begin{aligned}
&\dot{\varepsilon}_{cr} = A_4 \sinh[B_1(\sigma - \sigma_{th0})(1-H)] \\
&H = k_1\bar{\rho} + k_2\bar{c} + k_3\left(\bar{r}_{n2} + \beta^{\frac{1}{2}}\bar{r}_d\right) \\
&\dot{\bar{r}}_{n2} = C_r(Q - \bar{r}_{n2})^{m3}(1 + \gamma_0\bar{\rho}^{m4}) \\
&\dot{\bar{r}}_d = -\frac{Cr1}{\bar{r}_d} \\
&\dot{\bar{c}} = -A_2(\bar{c} - \bar{c}_a)(1 + \gamma_0\bar{\rho}^{m4}) \\
&\dot{\bar{\rho}} = A_1(1 - \bar{\rho})|\dot{\varepsilon}_{cr}|^{m_1} - C_p\bar{\rho}^{m2} \\
&\dot{\sigma}_{n2} = C_a\dot{\bar{r}}_{n2}^{m5}\left(1 - \bar{r}_{n2}{}^{m6}\right) \\
&\dot{\sigma}_d = C_{a1}r_d^{m7}\,\dot{\bar{r}}_d \\
&\dot{\sigma}_{ss} = -C_{ss}|\dot{\bar{c}}|^{m_5}(\bar{c} - \overline{c_a}) \\
&\dot{\sigma}_{dis} = A_3 n\bar{\rho}^{n-1}\dot{\bar{\rho}} \\
&\sigma_y = \sigma_{ss} + \sqrt{\sigma_{n2}^2 + \sigma_d^2 + \sigma_{dis}^2}
\end{aligned}\right\} \quad \text{(A.2)}$$

where $\dot{\varepsilon}_{cr}$ is the creep strain rate, H is a microstructural-controlled creep variable. The variables, $\bar{r}_n$, $\bar{r}_d$, $\bar{c}$ and $\bar{\rho}$ are the normalised microstructural variables representing the new precipitate radius, dissolving precipitate radius, solute concentration and dislocation density. The normalised dislocation density is defined as: $\bar{\rho} = (\rho - \rho_i)/\rho_s$ [9], where ρ_i is the initial dislocation density and ρ_s is the saturated dislocation density of the alloy during creep-ageing. The variables, σ_{n2}, σ_d, σ_{ss} and σ_{dis} are the strength contributions to the yield strength (σ_y) of the alloy from new precipitates, dissolving precipitates, solutes and dislocations respectively. The initial conditions for initial value problem for creep-ageing of AA2050-T34 at 428 K [9] are presented in table A2.

Table A2. The initial conditions of this system at $t = 0$ for equation SET 2.

ε_{cr} (-)	$\bar{r}_{n2}$ (-)	$\bar{r}_d$ (-)	$\bar{c}$ (-)	$\bar{\rho}$ (-)	σ_{n2} (MPa)	σ_d (MPa)	σ_{ss}(MPa)	σ_{dis} (MPa)
0	0	1	0.978	10^{-6}	0	110	120	100

The material constants for creep-ageing of AA2050-T34 at 428 K, determined in [9], are presented in table A3.

Table A3. Determined material constants for creep-ageing of AA2050-T34 at 428 K.

$\bar{c}_a$ (-)	C_r (h^{-1})	Q (-)	m_3 (-)	C_a (MPa)	m_5 (-)	m_6 (-)	C_{r1} (h^{-1})	C_{a1} (MPa)
0.316	0.108	1.1	1.25	180	0.65	6.5	0.108	120
m_7 (-)	A_2 (-)	C_{ss} (MPa)	m_8 (-)	A_1 (h^{-1})	m_1 (-)	m_2 (-)	C_p (-)	A_3 (-)
0.10	0.45	40	0.02	1.7	0.03	2.1	0.07	12
n (-)	A_4 (-)	B_1 (-)	k_1 (-)	k_2 (-)	k_3 (-)	γ_0 (-)	m_4 (-)	σ_{th0} (MPa)
0.8	4.5E-4	$1.32\text{x}10^{-2}$	0.618	0.622	0.226	0.08	1.28	18

SET 3: CDRX viscoplastic constitutive equations for aluminium alloys
A continuous dynamic recrystallisation (CDRX) based constitutive model was developed for hot deformation of aluminium alloys [10] as shown below:

$$\left.\begin{aligned}
&\dot{\varepsilon}_p = A_1 \sinh[A_2(|\sigma| - H - k)] \cdot S_{HAB}^{\gamma_d} \\
&\dot{H} = {}^1\!/_2\, B\bar{\rho}^{-0.5}\dot{\bar{\rho}} \\
&\dot{\bar{\rho}} = c_0 \left(\frac{S_{HAB0}}{S_{HAB}}\right)^{\gamma_S} (1-\bar{\rho})\dot{\varepsilon}_p - \alpha_1 \bar{\rho}^{c_1} - \alpha_2 S \bar{\rho}^{\gamma_\alpha} \\
&\dot{S}_{HAB} = c_2 S_{lab} \dot{\bar{\theta}}_{sub} \alpha_3 \bar{\rho}^{\gamma_{lab}} S_{lab}^2 \bar{\theta}_{sub}^{\gamma_\theta} \left(1 - \ln(\bar{\theta}_{sub})\right) - \alpha_2 \bar{\rho}^{\gamma_{HAB}} S_{HAB}^2 \\
&\dot{S}_{lab} = \alpha_4 \bar{\rho}^{\gamma_1} \dot{\varepsilon}_p - c_2 S_{lab} \dot{\bar{\theta}}_{sub} \alpha_3 \bar{\rho}^{\gamma_{lab}} S_{lab}^2 \bar{\theta}_{sub}^{\gamma_\theta} \left(1 - \ln(\bar{\theta}_{sub})\right) - \alpha_5 S_{lab} S_{HAB} \bar{\rho}^{\gamma_{HAB}} \\
&\dot{\bar{\theta}}_{sub} = \alpha_6 \bar{\rho}^{\gamma_2} \dot{\varepsilon}_p S_{lab}^2 \bar{\theta}_{sub} (\theta_r \bar{\theta}_{sub} - 1) \ln(n \cdot \bar{\theta}_{sub}) \\
&\dot{\sigma} = E\left(\dot{\varepsilon}_T - \dot{\varepsilon}_p\right) \\
&S = S_{HAB} + S_{lab} \\
&f_{HAB} = \tfrac{S_{HAB}}{S} \\
&d = \tfrac{2}{S_{HAB}}
\end{aligned}\right\} \quad \text{(A.3)}$$

where $n = \frac{\theta_c}{\theta_m}$, $\theta_r = \frac{\theta_c}{\theta_{sat}}$. The temperature-dependent parameters are given by the following temperature dependant relations:

$$E = E_0 \exp(-K_g T) \qquad \alpha_1 = c_{\alpha 1} \exp\left(-\frac{Q_a}{RT}\right) \qquad \alpha_4 = c_{\alpha_4} \exp\left(-\frac{Q_a}{RT}\right)$$

$$B = -c_B T + B_0 \qquad \alpha_2 = \frac{C_{\alpha_2}}{T} \exp\left(-K_g T - \frac{Q_b}{RT}\right) \qquad \alpha_5 = c_{\alpha_5} \exp\left(-\frac{Q_a}{RT}\right)$$

$$k = -c_k T + k_0 \qquad \alpha_3 = \frac{C_{\alpha_3}}{T} \exp\left(-K_g T - \frac{Q_b}{RT}\right) \qquad \alpha_6 = c_{\alpha_6} \exp\left(-\frac{Q_a}{RT}\right)$$

where, T is temperature in K. The initial values are presented in table A4, and the determined material constants used in the model are in table A5 [10].

Table A4. Initial conditions at $t = 0$ for equation SET 3.

σ (MPa)	ε_p (-)	$\bar{\rho}$ (-)	H (MPa)	S_{HAB} (μm^{-1})	S_{lab} (μm^{-1})	$\bar{\theta}_{sub}$ (-)
0	0	0.978	10^{-6}	0	110	120

Table A5. List of the constant values used for the set of CDRX equations for 7050 Al alloy.

A_1 (s^{-1})	A_2 (MPa^{-1})	R (J mol^{-1}K^{-1})	K_g(-)	c_0(-)	c_1(-)	c_2(-)	γ_1(-)
8.2x10^{-4}	0.15	8.31	5.40x10^{-4}	15.00	1.15	0.70	0.70
γ_2 (-)	γ_s (-)	γ_d (-)	γ_θ (-)	γ_{lab} (-)	γ_{HAB} (-)	γ_α (-)	n (-)
0.15	5.00	0.01	6.18	0.77	2.10	4.20	0.75
$c_{\alpha 1}$ (s^{-1})	$c_{\alpha 2}$ (μmKs^{-1})	$c_{\alpha 3}$ (μmKs^{-1})	$c_{\alpha 4}$(μm^{-1})	$c_{\alpha 5}$ (μm^{-1})	$c_{\alpha 6}$ (μm^2)	Q_a (J mol^{-1})	Q_b (J mol^{-1})
38.11	2.92x10^2	1.46x10^7	14.15	2.00x10^3	1.61x10^5	1.78x10^4	1.34x10^4
E_0 (MPa)	θ_c (-)	θ_m (-)	θ_{sat} (-)	c_B (MPaK^{-1})	c_k(MPaK^{-1})	B_0 (MPa)	k_0 (MPa)
7x10^4	15.00	20.00	6.00	0.40	0.14	2.96 x10^2	1.12x10^2

References

[1] Cao J, Lin J, and Dean T 2008 An implicit unitless error and step-size control method in integrating unified viscoplastic/creep ODE-type constitutive equations *International Journal for Numerical Methods in Engineering* **73**(8) 1094-1112
[2] Lush A, Weber G, and Anand L 1989 An implicit time-integration procedure for a set of internal variable constitutive equations for isotropic elasto-viscoplasticity *International Journal of Plasticity* **5**(5) 521-549
[3] Cormeau I 1975 Numerical stability in quasi-static elasto/visco-plasticity *International Journal for Numerical Methods in Engineering* **9**(1) 109-127
[4] Shampine L and Reichelt M 1997 The matlab ode suite *SIAM Journal on Scientific Computing* **18**(1) 1-22
[5] Petzold L 1983 Automatic selection of methods for solving stiff and nonstiff systems of ordinary differential equations *SIAM Journal on Scientific and Statistical Computing* **4**(1) 136-148
[6] Hairer E and Wanner G 1991 *Solving ordinary differential equations II: Stiff and differential-algebraic problems* (Springer series in computational mathematics). Springer, 2010, p. 614.
[7] Cash J 2003 Efficient numerical methods for the solution of stiff initial-value problems and differential algebraic equations *Proceedings of the Royal Society of London. Series A: Mathematical, Physical and Engineering Sciences* **459** 2032 797-815
[8] Lin J 2015 *Fundamentals of materials modelling for metals processing technologies: theories and applications* London: Imperial College Press
[9] Li Y, Shi Z, Lin J, Yang Y, and Rong Q **2017** Extended application of a unified creep-ageing constitutive model to multistep heat treatment of aluminium alloys *Materials & Design* **122** 422-432
[10] Li Y, Gu B, Jiang S, Liu Y, Shi Z, and Lin J 2020 A CDRX-based material model for hot deformation of aluminium alloys *International Journal of Plasticity* **134** 102844
[11] Ganapathy M, Li N, Lin J, and Bhattacharjee D 2020 A feasibility study on warm forming of an as-quenched 22MnB5 boron steel *International Journal of Lightweight Materials and Manufacture* **3**(3) 277-283
[12] Hairer E, Norsett S, and Wanner G 1993 *Solving ordinary, differential equations i, nonstiff problems* (Springer Series in Computational Mathematics). Springer, Berlin, Heidelberg p. 528
[13] Bonaventura L and Rocca A 2017 Unconditionally strong stability preserving extensions of the TR-BDF2 method *Journal of Scientific Computing* **70**(2) 859-895